engineering proceedings

MDPI

Proceeding Paper

The Emergence of Microneedle-Based Smart Sensor/Drug-Delivery Patches: A Scaling Theory Defines the Tradeoff between the Response Time and the Limits of Detection †

Marco Fratus and Muhammad A. Alam *

Elmore Family School of Electrical and Computer Engineering, Purdue University, West Lafayette, IN 47907, USA; mfratus@purdue.edu

* Correspondence: alam@purdue.edu

† Presented at the 2nd International Electronic Conference on Chemical Sensors and Analytical Chemistry, 16–30 September 2023; Available online: https://csac2023.sciforum.net/.

Abstract: Smart, ultra-scaled, always-on wearable, and implantable (WI) sensors are an exciting frontier in personalized medicine. These sensors integrate sensing and actuation capabilities, enabling real-time analyte detection for on-demand drug delivery, akin to a biological organ. The microneedle (MN)-based patch serves as a critical novel interface element in this system. It is inexpensive, minimally invasive, and safe, showing promise in glycemic management and insulin therapy in laboratory and animal studies. However, the current design of MNs relies primarily on empirical approaches, with significant challenges. These challenges include potential diffusion delays that may impede time-critical drug intervention and an iterative design process lacking a clear understanding of the tradeoff between the response time and the limits of detection. In this paper, we introduce the first predictive framework for MN sensors, based on physical scaling laws and biomimetic concepts. Our framework is supported by experimental and numerical validations, establishing analytical scaling relationships that capture the fundamental workings of hollow and porous-swellable MN sensors. It quantifies essential performance metrics like the 'response time (RT)' and the 'limit of detection (LOD)' while assessing the tradeoffs associated with various geometrical and physical parameters of the MN technology. As a result, our model provides a universal framework for interpreting/integrating the experimental findings reported by laboratories worldwide. By leveraging this predictive framework, researchers can advance the development and optimization of MN sensors, leading to improved performance and expanded applications in the field of wearable and implantable technologies.

Keywords: wearable and implantable sensors; modeling; scaling; microneedle; amperometry; response time; sensitivity; limit of detection; mechanics of insertion

Citation: Fratus, M.; Alam, M.A. The Emergence of Microneedle-Based Smart Sensor/Drug-Delivery Patches: A Scaling Theory Defines the Tradeoff between the Response Time and the Limits of Detection. *Eng. Proc.* **2023**, *48*, 29. https://doi.org/10.3390/CSAC2023-14906

Academic Editor: Nicole Jaffrezic-Renault

Published: 26 September 2023

1. Introduction

Smart healthcare, powered by ultra-scaled, and always-on digital electronics and wearable and implantable (WI) sensors, marks an exciting frontier in modern medicine. Technological advancements, including microfabrication, miniaturization, portability, low power, and cost-effectiveness, have shifted testing sites from traditional laboratories to "under or on skin" platforms [1–4].

Traditional devices developed for laboratory-based measurements face inherent limitations [5]: expensive tests, limited access in poorer communities, obtaining a single data point per test, and significant delays related to sample collection, laboratory reports, and therapy. Despite promoting point-of-care (POC) diagnostics as a complementary approach, these limitations persist, hindering independent and continuous monitoring of chronic diseases like diabetes and blood pressure. For them, indeed, highly trained technicians and self-disciplined patients are still required to run measurements or deliver drugs as needed, impeding accurate timely interventions.

A promising solution to these healthcare needs lies in closed-loop WI systems, integrating smart-sensing-controller–therapeutic interaction, as shown in Figure 1a. This revolutionary paradigm combines accurate sensing modalities with power transfer technology, data communication infrastructure, and machine learning algorithms, enhancing theragnostics. Skin-worn tattoos, patches, and textiles with wearable and implantable technology, along with actuating systems like brain and muscle stimulators or drug injectors, enable uninterrupted monitoring and immediate on-demand corrective therapies.

Microneedle (MN)-based patches, shown in Figure 1b, are part of WI systems, offering minimally-invasive analyte monitoring and drug delivery over several weeks [6,7]. These patches with short microneedles (a few hundred micrometers) can absorb analyte molecules or deliver drugs into the dermis. Compared to traditional hypodermic needles, MNs are less invasive and less painful due to fewer pain receptors in the dermis [8,9]. Moreover, the interstitial fluid (ISF) within the dermis contains valuable biomarkers like glucose, lactate, sodium ions, and others [10,11].

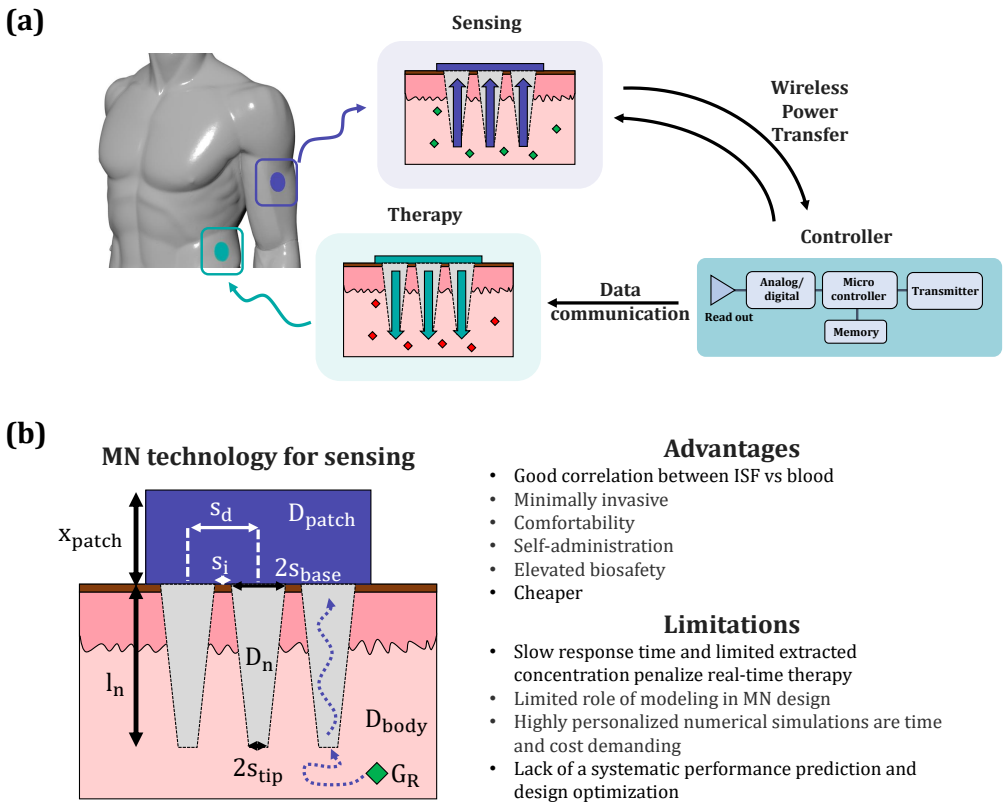

Figure 1. (**a**) Illustration of a closed-loop system (sensing, controller, and therapy) integrating microneedle (MN) technology for a wearable and implantable (WI) device. (**b**) Illustration of the geometric and physical properties of an MN-based patch, given an analyte concentration of interest in the dermis G_R. On the right, advantages and current limitations of the MN technology. l_n, s_{tip}, s_{base}, and s_d are the MN length, tip and base half widths, and inter-distance, respectively. x_{patch} is the patch thickness, and D_{patch}, D_n, and D_{body} are the analyte diffusivity in the patch, MN, and body, respectively.

The combination of disease diagnostics and drug delivery makes MN platforms ideal for closed-loop applications such as glycemic management and insulin therapy [12–14]. In traditional 'open-loop' operations, a patient performs glucose measurements and insulin pump therapy. In contrast, a smart MN patch integrates autonomous glucose measurement, data transmission to a controller algorithm, and autonomous therapeutic insulin delivery, forming a more efficient 'closed-loop' system.

2. Challenges and Limitations of MN Technology

The number of publications in MN-related areas has been growing exponentially over the past 20 years, with more than 80% of these publications focusing on experimental systems and fabrication protocols [15]. Despite significant progress in the field, the current design and optimization of MN systems involve costly and time-consuming iterative design of experiments. Researchers have explored a range of MN technologies, such as porous, swellable, and dissolvable platforms, alongside traditional hollow MNs, to achieve continuous monitoring with minimized sensor response delay and maximize the extracted concentration. Numerical analysis tools, such as finite element methods with COMSOL Multiphysics software, have limitations in efficiently exploring the vast design space associated with MN geometry and material parameters. The lack of universal scaling functions derived from numerical simulations makes it challenging to transfer insights from one design to another, hindering the systematic design and optimization of MN-based systems.

While a theory for therapeutic drug delivery has been developed [16], a comprehensive physics-based model for sensing optimization mediated by MNs is still missing. Without such a theory, it is difficult, if not impossible, to minimize the response time and maximize the extracted analyte concentration (limit of detection, LOD) for an optimized and efficient closed-loop system.

To address this gap, our work focuses on developing a generalized physics-based model for the in vivo operation of hollow, porous, and swellable (P−S) MN-based patches. Through validation against numerical simulations and experimental data, our theory establishes the foundation for the MN-related framework and provides strategies for designing and optimizing MN systems within the closed-loop theragnostic scenario. Moreover, the generality of the MN scaling theory makes it applicable to a broader range of applications, including electrochemical or optical sensors, enzymatic or nonenzymatic processes, in vitro and in vivo measurements, sensing, and actuation mechanisms.

3. A Scaling Theory of the Response Time and the Limit of Detection

3.1. Specific Design Challenges

- Wearable sensing devices require continuous and effective operation, necessitating real-time tracking of analyte concentrations. However, integrating MNs into wearable patches poses challenges due to analyte diffusion from the interstitial fluid (ISF) to the sensing site. This diffusion causes inherent delays in the sensor response (response time) and reduces the detectable analyte concentration (LOD) (Figure 2a), hindering an immediate closed-loop therapeutic response.
- Integrating fluid-absorbing MNs into electrochemical enzyme-based patches for on-site analysis adds complexity. Decoupling the impact of individual MN and enzymatic parameters on overall sensor performance proves to be a challenging task.
- Unlike hollow MNs, which absorb ISF across their tip aperture, P−S MNs enhance ISF absorption across their lateral surface, leading to a significant reduction in the response time and increased extracted analyte concentration (Figure 2). However, a theory comparing different MN technologies and quantifying this enhancement is currently missing.

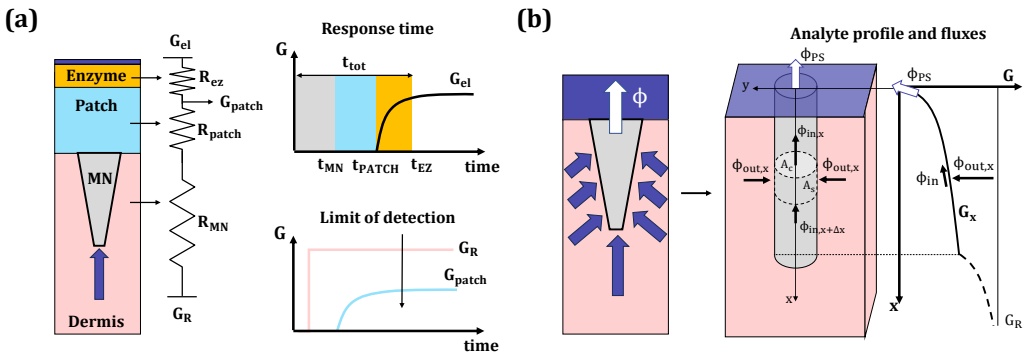

Figure 2. (**a**) Illustration of a hollow MN-based enzymatic sensor, and corresponding modeling in terms of electrical circuitry. Hollow MNs suffer from an intrinsic lag time t_{tot}; the total response is the sum of transport time across the MN (t_{MN}), sensor patch (t_{PATCH}), and enzyme kinetics (t_{EZ}). Also, given a fixed G_R (pink line), the accumulated analyte concentration in the patch (blue line, G_{patch}) is strongly suppressed, degrading the limit of detection (LOD). (**b**) Illustration of porous and swellable (P−S) cylindrical MN absorbing biofluid across the later surface and the corresponding modeling. We applied a balance of fluxes for an MN slice at distance x from the base aperture to derive the the theory of the analyte profile G_x (shown on the right) and the extracted flux Φ_{PS}.

3.2. Theoretical Framework of Hollow Microneedles

First, we derive a generalized framework to quantify the geometry-dependent response delay and LOD observed in hollow-type MN sensors. Here, the MNs are integrated in an enzymatic wearable patch with the sensing site (electrode) on the upper end of the patch, as shown in Figure 2a. We model the analyte extraction across MN tip and base as ion uptake by bacteria and gas flow across leaves the stomata [17] and molecule transport along MN length as the spreading resistance of a point contact [18]. It can be shown that the overall response time t_{tot} is the sum of individual contributions from the MN, patch, and enzymatic reaction:

$$t_{tot} = t_{MN} + t_{PATCH} + t_{EZ}, \quad (1)$$

where t_{MN} and t_{PATCH} are the turn-on delay times of analyte transport through the MN and sensor patch, and t_{EZ} is the effective time resulting from the diffusion and reaction in the enzyme layer, shown in Figure 2a. To quantify the time components, we approximate each sensor domain as a diffusive resistor R $[s \cdot m^{-3}]$ and multiply it by the corresponding transported ISF volume V [19]. To generalize the theory, we express the geometry-dependent components of (1), namely $l_n, s_{base}, s_{tip}, s_i$, in terms of scaled variables, $r_T = \frac{l_n}{s_{tip}}$, $r_B = \frac{l_n}{s_{base}}$, $r_i = \frac{l_n}{s_i}$, where l_n, s_{tip}, s_{base} are the MN length, half width of MN tip, and base apertures, respectively, s_i is the MN inter-base distance:

$$t_{MN} = R_{base}V_{base} + R_nV_n + R_{tip}V_{tip} = f(r_T, r_B, r_i, D_{body}, D_n, D_{patch}), \quad (2)$$

$$t_{PATCH} = R_{patch}V_{patch} = f(x_{patch}, D_{patch}), \quad (3)$$

$$t_{EZ} = \text{diffusion} - \text{limited } (t_{MN}, t_{PATCH}) \text{ vs reaction} - \text{limited (reaction rates)}. \quad (4)$$

Here, x_{patch} is the patch thickness, D_{body}, D_n, D_{patch} are the analyte effective diffusivity in the dermis, MN, and patch, respectively. The parameter t_{EZ} results from the competition of the analyte supply from the dermis (transport-limited) and enzyme kinetics (reaction rates).

Second, we quantify the averaged analyte concentration extracted in the patch (G_{patch}), given a fixed concentration in the dermis G_R, see Figure 2a. Regardless of the transduction mechanism (colorimetric, electrochemical, etc.), the accumulated G_{patch} is a critical parameter related to the minimum signal level set by the noise limit (LOD); since the G_{patch} may degrade below the noise limit along the diffusive path to the sensing site, the sensor may not register the analyte fluctuations in the skin and, thus, fail to deliver the appropriate

amount of drug. To determine G_{patch}, we assume steady state conditions and apply flux continuity among the enzyme, patch, and MN [19]:

$$\frac{G_{patch}}{G_R} \propto \frac{R_{ez} + \frac{R_{patch}}{2}}{R_{base} + R_n + R_{tip}}. \tag{5}$$

3.3. Theoretical Enhancement of Porous and Swellable Microneedles

For a faster closed-loop sensing and therapy, several approaches have been experimentally proposed, including the integration of P−S MNs in wearable patches [6,7,20,21]. Here, we derive a universal scaling relationship for P−S MNs and quantify their flux enhancement against hollow MNs. Ideally, given an arbitrary MN technology, the absorbing flux across the MN base aperture should be maximized for superior performance; a higher flux would absorb a higher analyte concentration in a shorter time to satisfy timely monitoring restrictions and minimum signal-to-noise ratio levels.

Although the theory can be generalized for an arbitrary geometry, we assume a cylindrical, homogeneous, isotropic MN, as shown in Figure 2b. First, we apply a flux balance in a slice of the MN at a distance x from the base:

$$\Phi_{in,x+\Delta x} A_c - \Phi_{in,x} A_c + \Phi_{out,x} A_s = 0, \tag{6}$$

where the concentration-dependent flux Φ is the gradient of analyte concentration, and A_c and A_s are the crossectional and lateral surface areas of the slice. The steady state solution of (6) gives the analyte profile G_x within the MN, assuming a fully absorbing MN base aperture ($G_{x=0} = 0$), see Figure 2b:

$$\frac{G_x}{G_R} = 1 - \frac{\cosh(m(l_n - x)) + H \sinh(m(l_n - x))}{\cosh(ml_n) + H \sinh(ml_n)}, \tag{7}$$

where s is the MN radius, $m \equiv \sqrt{\frac{2h_T}{sD_n}}$, with h_T being an empirical geometry-dependent coefficient regulating the analyte transfer between the MN and dermis, and $H = \frac{h_T}{mD_n}$.

Second, to evaluate the extraction efficiency of a P−S MN (Γ_{PS}), we normalize the flux at the base of MN aperture ($\Phi \propto D_n \frac{dG_x}{dx}$ at $x = 0$):

$$\Gamma_{PS} = r_h \frac{\sinh(r_h) + \frac{1}{2} r_g r_h \cosh(r_h)}{\cosh(r_h) + \frac{1}{2} r_g r_h \sinh(r_h)}, \tag{8}$$

where

$$r_h = ml_n \equiv \sqrt{h_T / \left(\frac{sD_n}{2l_n^2}\right)}, \tag{9}$$

$$r_g \equiv \frac{s}{l_n}. \tag{10}$$

Here, the parameter r_h encapsulates the geometric and physical properties of MN and the surrounding environment, thereby dictating the P−S ability to absorb analytes from the dermis. To compare the performance of the P−S and hollow technologies, we derive a similar relationship for hollow MNs at the base aperture of the MN:

$$\Gamma_H \approx \frac{1}{1 + \frac{D_n}{D_{body}} r_g}. \tag{11}$$

The ratio Γ_{PS}/Γ_H shows the theoretical enhancement in extracting the flux between the P−S MNs and hollow MNs.

4. Results

4.1. Impact on the Response Time and the Limit of Detection

Validated against COMSOL-based simulations, Figure 3a shows the impact of l_n on the response time (left, (1)) and the limit of detection (right, (5)) for a hollow MN-based patch. As expected, the theory predicts a tens of minutes to tens of hours lag time affecting the sensing operation of MN-based patches, depending on the sensor design. The diffusion time across the patch (t_{PATCH}, (3)) and the enzyme-related delay (t_{EZ}, (4)) set the critical limit of the performance. Overall, a longer MN would increase the transport time, degrading the closed-loop efficiency and suppressing the absorbed analyte concentration. Although not reported, a similar approach can be applied to predict the impact of other geometric and physical properties (MN apertures, MN material, and patch thickness) on sensor performance.

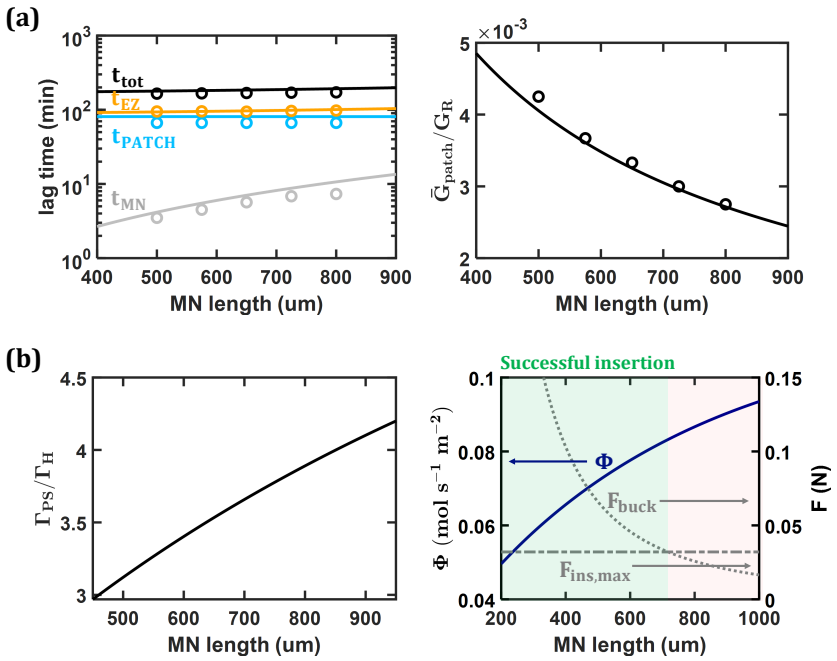

Figure 3. (**a**) COMSOL-based numerical validation of hollow MNs. Impact of MN length on (left) individual components of the total response time and on (right) the absorbed glucose concentration. The solid line is the theory, and the circles are the numerical results. (**b**) Analytical prediction for P−S MNs. Impact of the MN length on (left) the enhancement factor between P−S and hollow MNs and (right) on the tradeoff between the sensor performance (absorbed flux, blue line) and the mechanical requirements (dotted and dashed grey lines).

4.2. Enhancement and Limitations for Porous and Swellable Microneedles

Figure 3b shows the impact of l_n on the enhancement factor between P−S and hollow MNs ((8), (11), left) and on the tradeoff between the extracted flux and mechanical constraints for a P−S MN (right). Unlike a hollow MN, a P−S MN benefits from a longer MN, because of the enhanced surface area absorbing biofluid, see Figure 3a (right). The enhancement factor introduced by l_n is between 3 and 4; yet, by varying other geometric and physical variables (MN radius, diffusivity, etc.), it can achieve a factor of 6. Despite the significant benefits in performance, P−S MNs suffer from a weaker mechanical strength, limiting their skin insertion. Figure 3b shows that the tradeoff between the performance and mechanical constraints defines a 'window design' for P−S MNs. To successfully insert the MNs, a margin of mechanical safety ($F_{ins,max} < F_{buck}$, buckling limit higher than the maximum force supported by the MN) should be guaranteed, see [22]. While a longer MN maximizes the extracting flux Φ, it may cause mechanical failure ($F_{ins,max} > F_{buck}$);

therefore, there exists an optimized length satisfying both performance and mechanics at $F_{ins,max} = F_{buck}$.

5. Conclusions

We have developed a generalized theoretical framework for hollow and P−S MNs integrated into wearable patches as part of a comprehensive predictive model for personalized, autonomous, and independent theragnostics. Our theory quantifies sensor performance, including the response time and extracted analyte concentration, based on the geometric and physical properties of the sensor. We also identified the fundamental limitations of hollow MNs and predicted an enhancement factor introduced by P−S MNs, albeit with a tradeoff of weaker mechanical strength.

The model can be generalized to analyze novel MN technologies for an improved response time. For instance, the integration of sensing sites (electrodes) within MNs accelerates the detection by reducing the transport time [23]. Despite the potential degradation due to biofouling, the approaches involving functionalized MN surfaces reduce the response time by directly exposing sensing sites to analyte fluctuations in the dermis [24].

For a comprehensive analysis, the model should incorporate considerations of mechanical failure, inflammation, and biocompatibility-related concerns of MNs. More generally, by including a sensing-to-therapy algorithm and a theory for drug delivery, we would be able to provide a comprehensive framework for a systematic optimization of MN-based systems.

Author Contributions: Conceptualization, M.F. and M.A.A.; data curation, M.F.; methodology, M.F. and M.A.A.; theoretical derivation, M.F. and M.A.A.; model fitting, M.F.; validation, M.F.; visualization, M.F.; writing - original draft preparation, M.F.; writing - editing and review, M.A.A.; supervision, M.A.A. All authors have read and agreed to the published version of the manuscript.

Funding: This work was funded by Eli Lilly & Company. We thank Michelle Pearson for coordinating the operations between the Alam group and Eli Lilly & Company. The work was also supported by the Jai N. Gupta Endowed Chair Fund for Alam.

Institutional Review Board Statement: Not applicable.

Informed Consent Statement: Not applicable.

Data Availability Statement: The data that support the findings of this study are available within the article. The code is available on request.

Acknowledgments: The authors gratefully acknowledge discussions with Jongcheon Lim, Jim Nolan, Emilee Madsen, Yumin Dai, Chi Hwan Lee (Purdue University), Hugh Lee (Purdue University), and Jacqueline C. Linnes (Purdue University).

Conflicts of Interest: The authors declare no conflict of interest.

References

1. Fratus, M.; Alam, M.A. Universal scaling theory of electrochemical immunosensors: An analytical approach to define and compare performance metrics. *Appl. Phys. Lett.* **2023**, *122*, 054102. [CrossRef]
2. Heikenfeld, J.; Jajack, A.; Feldman, B.; Granger, S.W.; Gaitonde, S.; Begtrup, G.; Katchman, B.A. Accessing analytes in biofluids for peripheral biochemical monitoring. *Nat. Biotechnol.* **2019**, *37*, 407–419. [CrossRef] [PubMed]
3. de-la Fuente-Robles, Y.M.; Ricoy-Cano, A.J.; Albín-Rodríguez, A.P.; López-Ruiz, J.L.; Espinilla-Estévez, M. Past, Present and Future of Research on Wearable Technologies for Healthcare: A Bibliometric Analysis Using Scopus. *Sensors* **2022**, *22*, 8599. [CrossRef] [PubMed]
4. Friedel, M.; Thompson, I.A.P.; Kasting, G.; Polsky, R.; Cunningham, D.; Soh, H.T.; Heikenfeld, J. Opportunities and challenges in the diagnostic utility of dermal interstitial fluid. *Nat. Biomed. Eng.*, **2023**, 1–15. [CrossRef]
5. Alam, M.A.; Saha, A.; Fratus, M. Reliable sensing with unreliable sensors: Rethinking the theoretical foundation of field-deployed wearable/implantable/environmental sensors. *Innov. Emerg. Technol.* **2022**, *9*, 2240003. [CrossRef]
6. Zhang, X.; Gan, J.; Fan, L.; Luo, Z.; Zhao, Y. Bioinspired Adaptable Indwelling Microneedles for Treatment of Diabetic Ulcers. *Adv. Mater.* **2023**, *35*, 2210903.
7. Sang, M.; Cho, M.; Lim, S.; Min, I.S.; Han, Y.; Lee, C.; Shin, J.; Yoon, K.; Yeo, W.H.; Lee, T.; et al. Fluorescent-based biodegradable microneedle sensor array for tether-free continuous glucose monitoring with smartphone application. *Sci. Adv.* **2023**, *9*, eadh1765.

8. Ribet, F.; Bendes, A.; Fredolini, C.; Dobielewski, M.; Böttcher, M.; Beck, O.; Schwenk, J.M.; Stemme, G.; Roxhed, N. Microneedle Patch for Painless Intradermal Collection of Interstitial Fluid Enabling Multianalyte Measurement of Small Molecules, SARS-CoV-2 Antibodies, and Protein Profiling. *Adv. Healthc. Mater.* **2023**, *12*, 2202564.
9. Xu, J.; Yang, B.; Kong, J.; Zhang, Y.; Fang, X. Real-Time Monitoring and Early Warning of a Cytokine Storm In Vivo Using a Wearable Noninvasive Skin Microneedle Patch. *Adv. Healthc. Mater.* **2023**, *12*, 2203133.
10. Müller, M.; Cascales, J.P.; Marks, H.L.; Wang-Evers, M.; Manstein, D.; Evans, C.L. Phosphorescent Microneedle Array for the Measurement of Oxygen Partial Pressure in Tissue. *ACS Sens.* **2022**, *7*, 3440–3449.
11. Himawan, A.; Vora, L.K.; Permana, A.D.; Sudir, S.; Nurdin, A.R.; Nislawati, R.; Hasyim, R.; Scott, C.J.; Donnelly, R.F. Where Microneedle Meets Biomarkers: Futuristic Application for Diagnosing and Monitoring Localized External Organ Diseases. *Adv. Healthc. Mater.* **2023**, *12*, 2202066.
12. Ghoreishizadeh, S.S.; Moschou, D.; McBay, D.; Gonalez-Solino, C.; Dutta, G.; Di Lorenzo, M.; Soltan, A. Towards self-powered and autonomous wearable glucose sensor. In Proceedings of the 2018 25th IEEE International Conference on Electronics, Circuits and Systems (ICECS), Bordeaux, France, 9–12 December 2018; pp. 701–704. [CrossRef]
13. Boughton, C.K.; Hovorka, R. New closed-loop insulin systems. *Diabetologia* **2021**, *64*, 1007–1015. [CrossRef] [PubMed]
14. Doyle, F.J., III; Huyett, L.M.; Lee, J.B.; Zisser, H.C.; Dassau, E. Closed-Loop Artificial Pancreas Systems: Engineering the Algorithms. *Diabetes Care* **2014**, *37*, 1191–1197.
15. Yadav, P.R.; Han, T.; Olatunji, O.; Pattanayek, S.K.; Das, D.B. Mathematical Modelling, Simulation and Optimisation of Microneedles for Transdermal Drug Delivery: Trends and Progress. *Pharmaceutics* **2020**, *12*, 693. [CrossRef] [PubMed]
16. Avila, R.; Li, C.; Xue, Y.; Rogers, J.A.; Huang, Y. Modeling programmable drug delivery in bioelectronics with electrochemical actuation. *Proc. Natl. Acad. Sci. USA* **2021**, *118*, e2026405118.
17. Berg, H.C. *Random Walks in Biology*; Princeton University Press: Princeton, NJ, USA, 2018. [CrossRef]
18. Karmalkar, S.; Mohan, P.V.; Nair, H.P.; Yeluri, R. Compact Models of Spreading Resistances for Electrical/Thermal Design of Devices and ICs. *IEEE Trans. Electron Devices* **2007**, *54*, 1734–1743. [CrossRef]
19. Fratus, M.; Lim, J.; Nolan, J.; Madsen, E.; Dai, Y.; Lee, C.H.; Linnes, J.C.; Lee, H.; Alam, M.A. Geometry-defined Response Time and Sensitivity for Microneedle-based Amperometric Sensors. *IEEE Sens. J.* **2023**, *23*, 14285–14294. [CrossRef]
20. Zhang, J.; Li, H.; Albakr, L.; Zhang, Y.; Lu, A.; Chen, W.; Shao, T.; Zhu, L.; Yuan, H.; Yang, G.; et al. Microneedle-enabled therapeutics delivery and biosensing in clinical trials. *J. Control. Release* **2023**, *360*, 687–704. [CrossRef]
21. Li, X.; Xu, X.; Wang, K.; Chen, Y.; Zhang, Y.; Si, Q.; Pan, Z.; Jia, F.; Cui, X.; Wang, X.; et al. Fluorescence-Amplified Origami Microneedle Device for Quantitatively Monitoring Blood Glucose. *Adv. Mater.* **2023**, *35*, 2208820.
22. Kashaninejad, N.; Munaz, A.; Moghadas, H.; Yadav, S.; Umer, M.; Nguyen, N.T. Microneedle Arrays for Sampling and Sensing Skin Interstitial Fluid. *Chemosensors* **2021**, *9*, 83. [CrossRef]
23. Parrilla, M.; Vanhooydonck, A.; Johns, M.; Watts, R.; De Wael, K. 3D-printed microneedle-based potentiometric sensor for pH monitoring in skin interstitial fluid. *Sens. Actuators B Chem.* **2023**, *378*, 133159. [CrossRef]
24. Teh, F.; Teymourian, H.; Wuerstle, B.; Kavner, J.; Patel, R.; Furmidge, A.; Aghavali, R.; Hosseini-Toudeshki, H.; Brown, C.; Zhang, F.; et al. An integrated wearable microneedle array for the continuous monitoring of multiple biomarkers in interstitial fluid. *Nat. Biomed. Eng.* **2022**, *6*, 1214–1224. [CrossRef]